The 2010 IEEE/RSJ International Conference on
Intelligent Robots and Systems
October 18-22, 2010, Taipei, Taiwan

Development of a 3D Interactive Virtual Market System with Adaptive Treadmill Control

Haiwei Dong, Tatuo Oshiumi, Akinori Nagano and Zhiwei Luo, *Member, IEEE*

***Abstract*—As the computer vision and virtual reality (VR) technology become mature nowadays, there is a huge potential to connect VR with the real world. In this paper, a 3D interactive VR system with adaptive treadmill control is developed. The subject walks on the treadmill at will. Interaction force between feet and treadmill are measured to estimate the subject's intended walking speed. The treadmill belt velocity and 3D display adjust to the walking pace according to the subject's walking intention, which makes the subject feel that he (or her) is walking in the real market. The experiment shows that the control results are smooth, which verifies the validity of the whole system.**

I. Introduction

With the development of computer science, especially computer vision and virtual reality (VR) technology, more and more VR systems have come out. However, most of them were designed for computer games and special trainings, like medical training [1-2], social skill training [3]. In fact, the VR system can be much more valuable and useful when it is connected with real-world. Take service for the elderly people for example, the traditional service for the elderly people is non-interactive. For instance, since the physical strength of the elderly person is weak, their goods are delivered by express in normal cases. If things continue this way, the elderly people are lack of mental and physical exercises. Compared with the mentioned non-interactive service, VR interactive system can be designed in the following way that an elderly person takes walks in the VR world by taking steps on the real-world treadmill. Furthermore, he (or she) can buy things directly in the VR shops which connect with the selling system of the real shops. Such interactive service provides the elderly people with convenience and health, which is the final objective of our research. This paper is the very first step of the whole idea which develops a 3D interactive VR system with adaptive treadmill.

Actually, this paper concerns on the issue noted as locomotion interface which is defined as travelling through a virtual environment by subject's self-propulsion [4-5]. Here we list the researches relating with treadmill-style locomotion interface. The early work was done by Noma et al. who built a treadmill locomotion interface system ATLAS [6] where stance duration and body position are applied in PI control for driving the treadmill. In [7], Darken and Carmein. developed the first omini-directional treadmill to facilitate turning. In [8], Iwata and Yoshida built another two dimentional treadmill which employs twelve small treadmills to form a large belt. In [9-10], Hollerbach et al. designed two generaltions of treadmill-style locomotion interfaces named Sarcos Treadport which imitates slope by pushing or pulling a tether located at the back of the subject.

In this paper, when one subject walks on the treadmill, the force plate measures the forces in x, y, z directions exerted by the subject. Based on the sensor data, we estimate the subject's intended walking speed and adjust the velocity of the treadmill belts by it. Meanwhile the 3D projector goes on with the walking pace. Compared with previous treadmill-style locomotion systems, there are two characters of the system built in this paper. The first is that we use the human's intended walking speed to drive the treadmill. Specifically, we find a linear relation between force measurement and intended walking speed. Based on it, the speed control is simple as a linear computation. The second is that our system not only gives natural feeling of walking, but also gives natural sense of vision and hearing. The 3D display based on virtual reality and the ambient sounds of the environment make the subject have an immersed sense. In addition, the layout of shops is based on a real market located in Hokkaido Japan, which makes the whole system be much more realistic.

This paper is organized as follows. Section II illustrates the system construction and working mechanism. Section III proposes a velocity control scheme of the treadmill based on the skeleton model simulation results. Section IV presents the software structure and parameter settings of 3D display. Section V shows that the proposed approach is capable to control the treadmill velocity and 3D display well, which verifies the validity of the whole system. Section VI concludes the whole paper.

II. System Construction and Problem Formation

The system consists of three modules as centurial processing PC, Bertec treadmill and 3D stereoscopic display (Fig.1). When the subject walks on the treadmill, the dual force plates (placed under the treadmill) measure the force and moment signals in x, y, z directions as F_x, F_y, F_z, M_x, M_y, M_z and output them as analog signals. After amplifying them and doing analog-to-digital (A/D) conversion by LABVIEW data acquisition, the digital signals are transferred to centurial

Manuscript received March 5, 2010.

Haiwei Dong, Tatuo Oshiumi, Akinori Nagano and Zhiwei Luo are with the Graduate School of Engineering, Kobe University, Kobe, 657-8501, Japan (e-mail: haiwei@stu.kobe-u.ac.jp; oshiumi@cs11.cs.kobe-u.ac.jp; aknr-ngn@phoenix.kobe-u.ac.jp; luo@gold.kobe-u.ac.jp).

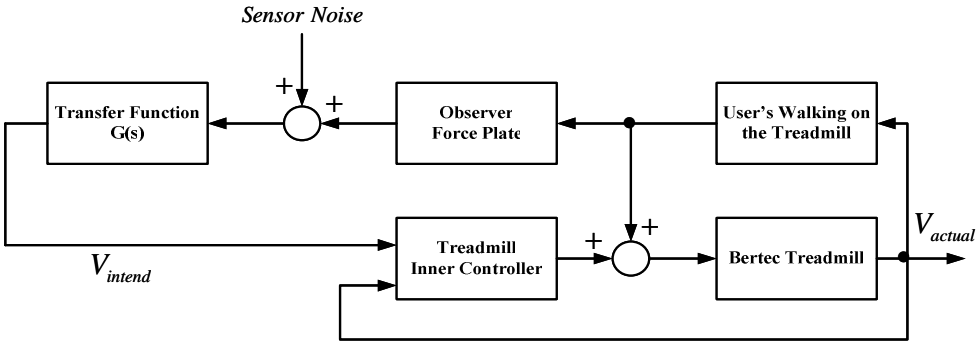

Fig.2 System block diagram. The treadmill has an inner controller with many feedback loops to control the speed of the belts. When the user walks on the treadmill, the force plate measures the forces and moments in x, y, z directions. By a transfer function $G(s)$, the desired walking speed of the user can be obtained from the sensor data.

processing PC. Based on the force signals, intended walking speed of the user is estimated. The estimated speed is used in two ways: one is to drive the two motors corresponding to left belt control, right belt control; the other is to drive the 3D virtual reality scene to move on.

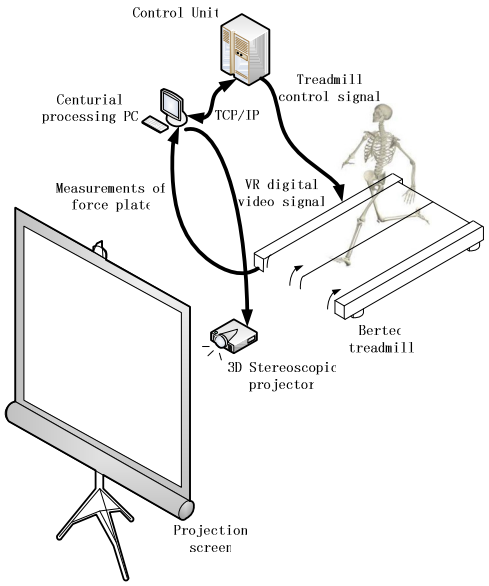

Fig.1. System construction. The system is composed of three modules including centurial PC, treadmill and 3D display.

The system block diagram is shown in Fig.2. From the viewpoint of control theory, the control plant is Bertec treadmill which is controlled by treadmill inner controller in the inner loop feedback. When the user walks on the treadmill, there is a noise adding to the control signal. It is noted that the control objective is to control the treadmill by the user's will. Hence, we establish an outer loop feedback between the user's intended walking speed V_{intend} and the treadmill inner controller. In this case, the force plate is chosen as the observer which measures the interactive forces between feet and treadmill. Besides of the sensor noise, we want to establish a relation between V_{intend} and the measurement data, i.e. recognize and identify the transfer function $G(s)$.

III. Bertec Treadmill Control

In this section, according to the walking simulation data, a critical feature which corresponds to the intended walking speed is obtained. By the least-squares regression method, the relation between the proposed ratio and intended walking speed is established.

A. Force Plate

First of all, let us define the standard coordinate system as that the positive y-direction points forward; x-axis points left when looking in the y-direction; and the z-axis is defined downwards by the right hand rule. The origin of the coordinate system is centered at the inner corner of the outer back roller support block of the corresponding (right or left) treadmill half.

Each half of Bertec dual belt treadmill incorporates an independent force plate measuring six load components: the three orthogonal components of the resultant force and three components of the resultant moment in the same orthogonal coordinate system. All the forces acting between the foot and the ground can be summed to yield a single ground reaction force F and a free torque vector T_z . The point of application of the ground reaction force on the plate is the center of pressure (CP). All the small reaction forces collectively exert on the surface of the plate at the CP. The point of application of the force and the couple acting can be readily calculated from the measured force and moment components independently on each half of the treadmill (Fig.3).

The two force plates are calibrated individually and the calibration matrix is stored digitally in the force plate. The voltage output of each channel is in a scaled form of the load with the units of N and N·m for the forces and moments, respectively. The scale factor for each channel for a gain of unity is given in the product data sheet supplied with the transducer. The force and moment values are calculated by multiplying the signal values with corresponding scale factors,

as given

$$\begin{bmatrix} F_x \\ F_y \\ F_z \\ M_x \\ M_y \\ M_z \end{bmatrix} = \begin{bmatrix} C_1 & & & & & \\ & C_2 & & & 0 & \\ & & C_3 & & & \\ & & & C_4 & & \\ & 0 & & & C_5 & \\ & & & & & C_6 \end{bmatrix} \begin{bmatrix} S_1 \\ S_2 \\ S_3 \\ S_4 \\ S_5 \\ S_6 \end{bmatrix} \quad (1)$$

where, F_x, F_y, F_z and M_x, M_y, M_z are the force and moment components in the force transducer coordinate system, in N and N.m, respectively. S_1, S_2, S_3, S_4, S_5 and S_6 are the output signals corresponding to the channels indicated by their subscripts, in volts, divided by the respective channel gain. The diagonal matrix composed of C_1, C_2, C_3, C_4, C_5, C_6 is the calibration matrix with units N/V for the force channels (C_1, C_2, C_3) and moment channels (C_4, C_5, C_6) [12].

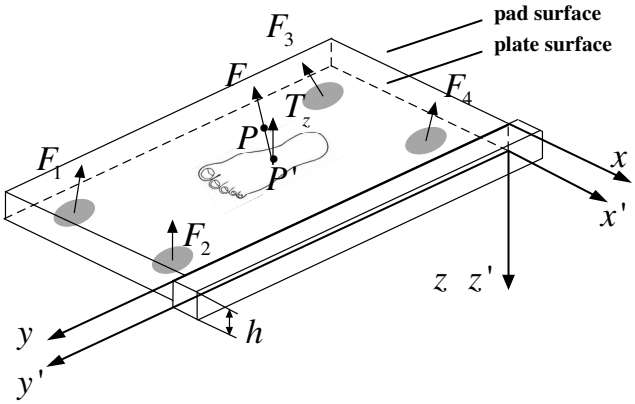

Fig.3 Force plate. There are four force sensors located at the bottom of the force plate. Finally, the force plate outputs forces and moments of F_x, F_y, F_z, M_x, M_y, M_z. The height of pad, denoted as h, is 0.15m.

B. *Characteristic Index* R_{yz}

The simulation was done by OpenSim 2.0. The skeleton model is 72.419 kg weight where red arrow, green arrow and blue arrow denote y, -z and -x directions, respectively (Fig.4). The model is composed of as many as 12 parts as torso, pelvis, femur-r, tibia-r, talus-r, calcn-r, toes-r, femur-l, tibia-l, talus-l, calcn-l and toes-l. In order to simulate the real human model better, 28 muscles forces and contact forces, etc. are also added in the model. It is noted that, because upper limbs are not be of crucial importance, the model was built without upper limbs for simplicity.

The simulation results show that in one dynamic circle, the force F_z is a bell-shape signal, and F_y is a sine-shape signal (Fig.5). We can explain the reason for curve shape of F_y and F_z as follows. When the foot gets in touch with the surface of treadmill, F_z increases very rapidly. At the same time, the foot has to make a break to adjust its speed to the velocity of the belt by friction. After break process, the foot applies a force with inverse direction to drive the leg to take a step, i.e. make a preparation for higher speed of leg in the next moment. It is noted that, compared with break process, F_y changes its direction at this time. Until now, the foot is on the treadmill all along. Hence, F_z maintains large (for a normal person with 70 kg weight, F_z is about 700 N). Finally, the body alternates the other foot to support body and F_z decreases very rapidly.

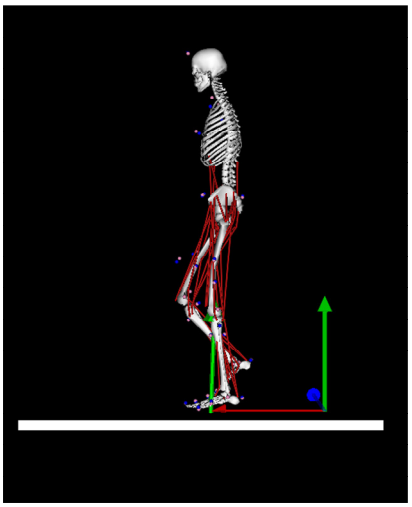

Fig.4 Human skeleton model. The coordinates system is set that red arrow, green arrow, blue arrow denote y, -z, -x directions, respectively.

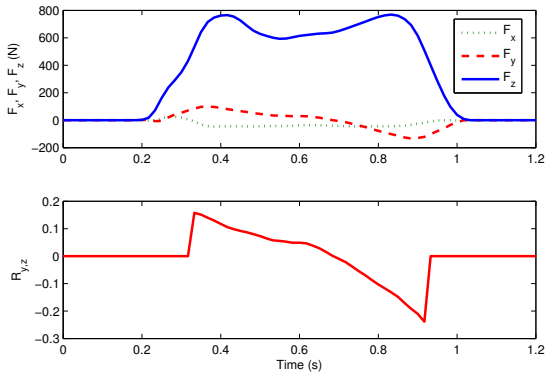

Fig.5 Forces between foot and ground. F_y is a sine-shape curve and F_z is a bell-shape curve. Hence, R_{yz} is a sine-shape curve.

Considering the fact that when F_z is large enough, one foot is firmly on the treadmill. We define a force ratio $R_{y,z}$ as

$$R_{y,z} = \begin{cases} \dfrac{F_y}{F_z} & F_z \geq \xi \\ 0 & others \end{cases} \quad (2)$$

where ξ is a threshold. In the normal cases, it is chosen that $\xi = \max\{F_z\} \times 80\%$. According to the curve shapes of F_y and F_z, the curve shape of $R_{y,z}$ is a composite signal of connection of sine-shape signals and zero signals (Fig.5).

Without loss of generality, the zero signals are ignored in analysis. $R_{y,z}$ becomes a composite signal of connection of numerous sine-shape signals with different magnitude. $R_{y,z}$ has a direct relation with the intended walking speed. When the user intends to speed up, $\|R_{y,z}\|_\infty$ becomes large. In other words, the envelope curve of $R_{y,z}$ determines the intended walking speed (Fig.6 (a)). The above illustration is roughly verified by the walking experiment when the treadmill velocity increases from 1.0 m/s to 1.6 m/s as shown in Fig.6 (b). Further verification is shown in the section of experiment.

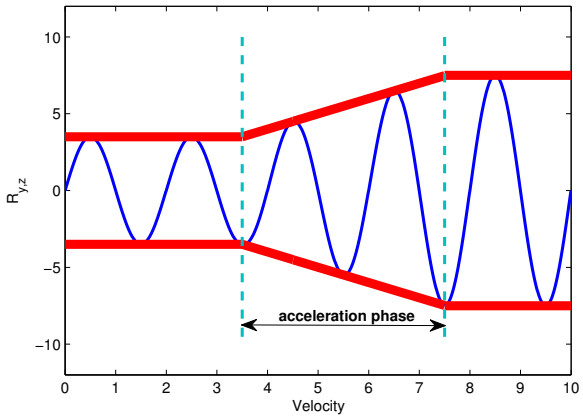

(a)

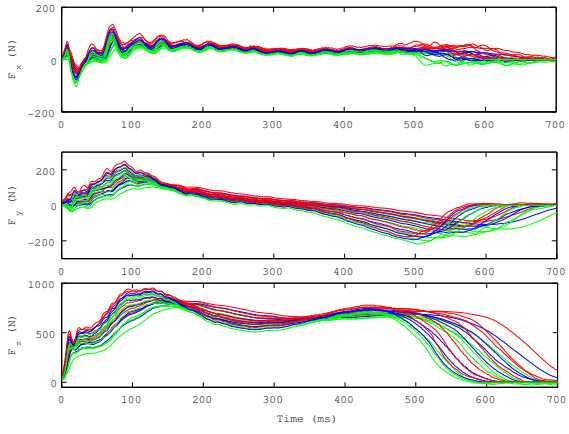

(b)

Fig.6 (a) In the acceleration phase, the origin equilibrium state with low speed transfers to a new equilibrium state with high speed. (b) With the increase of treadmill speed (from 1.0 m/s to 1.6 m/s), the magnitudes of F_x, F_y, F_z become large gradually.

C. *Least-squares Regression*

First of all, define the local peak value $R^+_{y,z}$ and local valley value $R^-_{y,z}$ of $R_{y,z}$ as

$$\begin{aligned} R^+_{y,z} &= \max_{0\le t\le T}\{R_{y,z}\} \\ R^-_{y,z} &= \min_{0\le t\le T}\{R_{y,z}\} \end{aligned} \tag{3}$$

where T is the period of $R_{y,z}$. Then we can get a sequence of measurements

$$(V_1, R^-_{y,z,1}), (V_2, R^-_{y,z,2}), \cdots, (V_n, R^-_{y,z,n}) \tag{4}$$

Assumed that $R^-_{y,z}$ is predicted as a function of V then one can model this situation by

$$R^-_{y,z} = f(V, \lambda) + \varepsilon \tag{5}$$

where λ is parameter vector. The random variable ε is independent of V and on average it is equal to zero, i.e. $E(\varepsilon) = 0$. We want to find f that fits the measurement data best and we define the loss function to measure the quality of the fit as

$$L = \left\| R^-_{y,z} - f(V, \lambda) - \varepsilon \right\|_2 \tag{6}$$

and we minimize it over all choices of parameter vector λ. To find the approximation function, we write

$$\frac{\partial L\left(R^-_{y,z}, f(V,\lambda), \varepsilon\right)}{\partial \lambda} = 0 \tag{7}$$

It is noted that, the above estimation solution is unbiased estimation since

$$\begin{aligned} E\left(R^-_{y,z} \mid V\right) &= E\left(f(x,\lambda) + \varepsilon \mid V\right) = f(x,\lambda) + E(\varepsilon \mid V) \\ &= f(x) + E(\varepsilon) = f(x) \end{aligned} \tag{8}$$

IV. Stereo Display

The virtual market display module is connected with other modules by TCP/IP protocol. Each time, the centurial processing PC collects the force measurements from the force plates. After system identification computation, the intended walking speed of the subject is estimated. Based on the estimated speed, the 3D display goes on.

The design of the virtual market is based on a real market located in Hokkaido, Japan. Thus, the environment has apparent Japanese characters. Right now, the market is designed as a north-south street with a length of 80 meters, which includes one traffic corner and numerous cross roads. There are 20 shops in all with 10 shops distributing on each side of the road. At the end of the road, there is a train station by entering which the program terminates (Fig.7).

The program was developed by Visual C++. In general, the utility toolkit GLUT was used for vision design and SDL library was used for sound design. For the vision design, the 3D models of shops, post office, etc. were constructed by Metasequoia which is a polygon modeler for 3DCG and game development. Specifically, everything is created as an assembly of several basic geometrical bodies. Each face of the

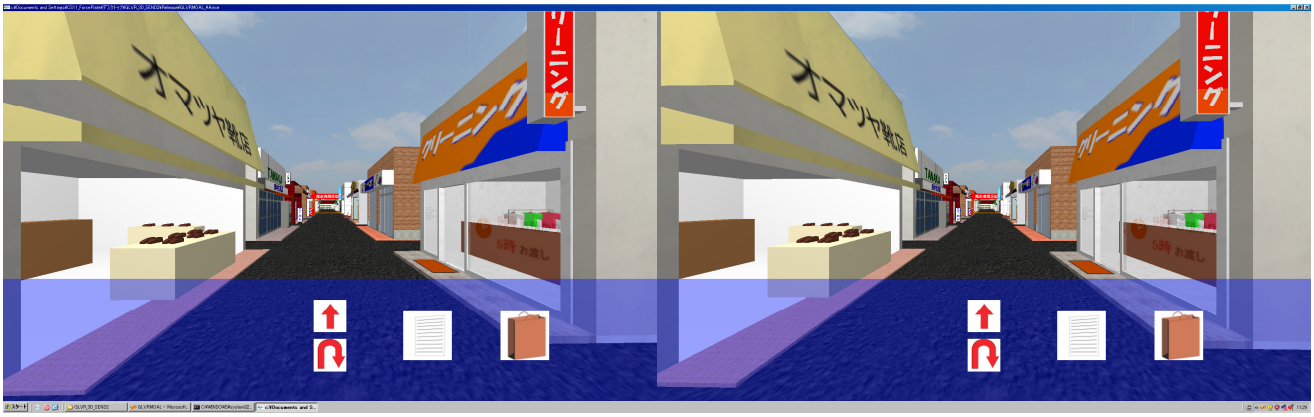

Fig.7 Binocular vision of 3D virtual shopping street. The market is designed based on a real market located in Hokkaido Japan. The virtual market is a north-south street with a length of 80 meters including one traffic corner and numerous cross roads.

composite unit is assigned a special texture. For example, the surface of ground is mapped with asphalt material; the surface of sky is mapped with cloud. Finally, the above generated 3D model data were used by the utility toolkit GLUT OpenGL directly. For the sound design, we used SDL-mixer library to create various sounds, like the footstep sound, the market sell voice, etc. Even at the place near the train station, the subject can hear the jingle of the train from the distance to the close.

In order to realize stereoscopic display, we have to configure the height of the viewpoint. Assuming that the average height of man is about 170 cm and of woman is about 160 cm, respectively, the height of viewpoint is compromised to be 165 cm. In practical application, the user wears a 3D eyewear. Actually, the 3D eyewear has two different eyeglasses which allow different polarized light pass separately. In such a way, the left and right eyes of the user see different images from its own viewpoint (Fig.7). In the system, papillary distance is set as 7 cm. Thus, the left and right optical lines of sight cross at 1 m before the user.

In addition, the system has many options. For example, the user can choose whether there is background music at the beginning of the program. Besides, the user also can choose different street to walk.

V. Experiment

In the experiment, the subject walks on the treadmill at will. Meanwhile, the VR shopping scene goes on with the intended walking speed. As the projector is a stereoscopic projector, by wearing a pair of 3D glasses, the subject have a more immersive and realistic experience (Fig.8). The program was written by three software packages as Visual C++, LabView and Matlab. The usage details of the software packages are shown as follows. The VR-related works, e.g. 3D display, is developed by Visual C++. The hardware-related works, like data acquisition, treadmill control, etc. were programmed by LabView. The computation-related works, e.g. least squares regression, were accomplished by Matlab.

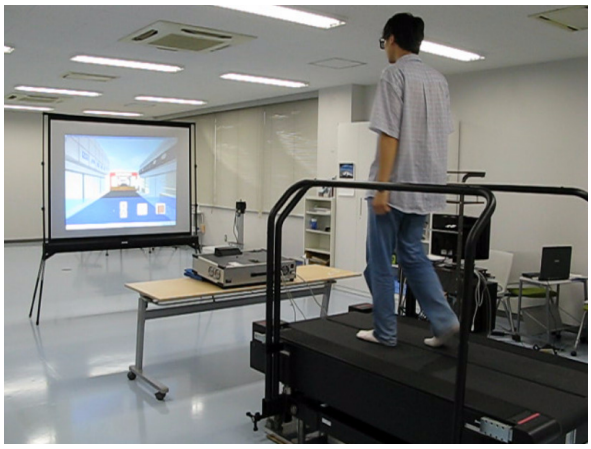

Fig.8 Experiment environment. The subject walks on the treadmill and meanwhile watching the 3D scene.

During the process, the communication between three modules is done by TCP/IP protocol. The sender is localhost (meaning “this computer”) which translates to the IP address 127.0.0.1 and the port is defined as 4000. In detail, when transferring speed signal to treadmill, the TCP/IP packet is shown in Table I.

TABLE I
TCP/IP Transfer Packet

Space	Meaning
U8	Format specifier (set to 0)
4*S16	Belt speed in mm/s
4*S16	Belt acceleration in mm/s^2
S16	Incline angle in 0.01 deg
4*S16	Belt speed complement (bit-inverted) in mm/s
4*S16	Belt acceleration complement (bit-inverted) in mm/s^2
S16	Incline angle complement (bit-inverted) in 0.01 degree
27*U8	Padding

(where <U|S> - U(nsigned)|S(igned) <8|16> - size in bits)

When the velocity of treadmill is set as 0.5 m/s, the forces F_x, F_y and F_z are shown in Fig.9. It shows that F_y is a sine-shape curve and F_z is a bell-shape curve, which verifies the simulation analysis in Section III, Part B.

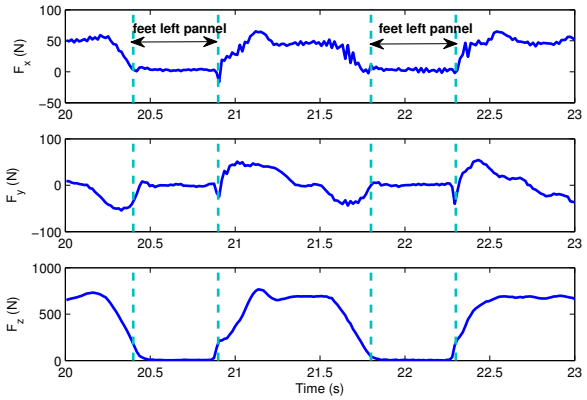

Fig.9 Measurement of F_x, F_y, F_z. The foot leaves the force plate in the time interval of $[20.4, 20.9]$ s and $[21.8, 22.3]$ s.

In order to do least-squares regression, we have to collect many observation samples. In the experiment, we compute $R_{y,z}$ ten times when the velocity varies from 0.1 m/s to 1.0 m/s. The observation results are shown in Table II.

TABLE II
OBSERVATION SAMPLES

Velocity (m/s)	$R^+_{y,z}$	$R^-_{y,z}$
0.1	0.0080	-0.0213
0.2	0.0310	-0.0353
0.3	0.0716	-0.0542
0.4	0.0622	-0.0695
0.5	0.0957	-0.0884
0.6	0.0872	-0.1172
0.7	0.1078	-0.0834
0.8	0.1126	-0.1224
0.9	0.1153	-0.1187
1.0	0.1841	-0.1421

By using the least-squares regression method in Section III, Part C, we obtained four types of regression models as linear, quadratic, cubic and 4th degree polynomial (Table III). The regressions are also shown in Fig.10 (a) and the residual statistics is shown in Fig.10 (b).

TABLE III
LEAST-SQUARES REGRESSION RESULTS

Regression Model	Results	Norm of Residuals
linear	$R^-_{y,z} = -0.13V - 0.011$	0.039887
quadratic	$R^-_{y,z} = 0.067V^2 - 0.2V - 0.00072$	0.034701
cubic	$R^-_{y,z} = -0.08V^3 + 0.19V^2 - 0.25V + 0.0022$	0.034094
4th degree polynomial	$R^-_{y,z} = -0.6V^4 + 1.1V^3 - 0.56V^2 - 0.097V - 0.0021$	0.031844

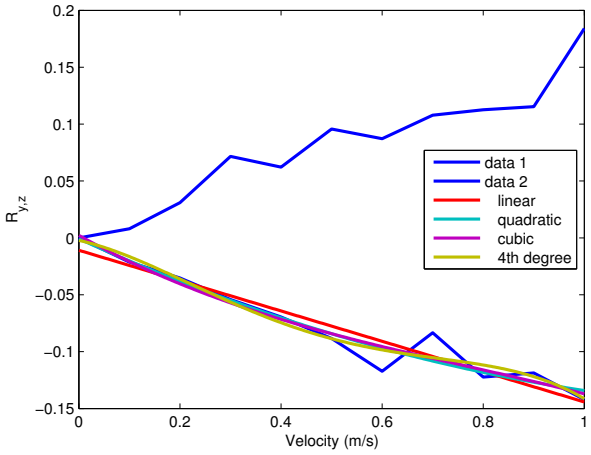

(a)

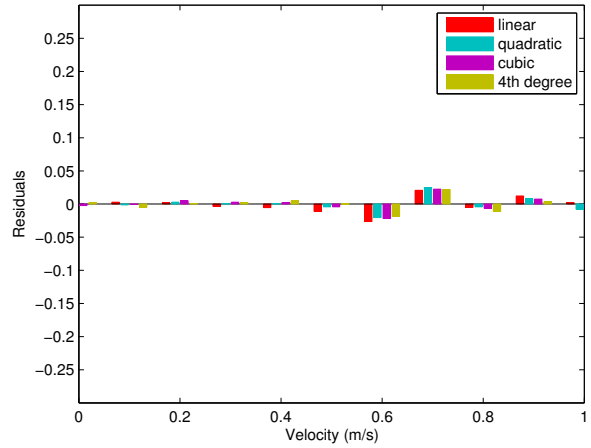

(b)

Fig.10 Least-squares regression. (a) Regression results of the four types of model as linear, quadratic, cubic and 4th-degree polynomial. (b) Residuals results of regression.

It is shown that the residual norms of the four types do not have big difference. Hence, we choose the simplest linear regression model to use. The proposed treadmill velocity control is obtained

$$V(k) = \begin{cases} V(k-1) & R^-_{y,z}(k) = 0 \\ -\left(R^-_{y,z}(k) + 0.011\right)/0.13 & others \end{cases} \quad (9)$$

There are many reasons, e.g. sensor noise, to cause computed velocity not smooth. In this paper, we choose a delay-line filter to overcome the problem. The filter is described by the difference function

$$V(k)=\frac{1}{4}\sum_{i=1}^{4}V(k-i) \tag{10}$$

There are also many low-pass filters, such as Butterworth filter, Chebyshev filter, Bessel filter, etc, which are available to be used considering the frequency of noise. Fig.11 (a) shows a complete dynamic walking process with acceleration motion, deceleration motion and uniform motion (i.e. constant velocity motion), where the solid line denotes velocity and dash line denotes F_y, respectively. Fig.11 (b) shows part views of acceleration motion, deceleration motion and uniform motion in the time interval $[28,34]$, $[55,65]$ and $[15,24]$, respectively.

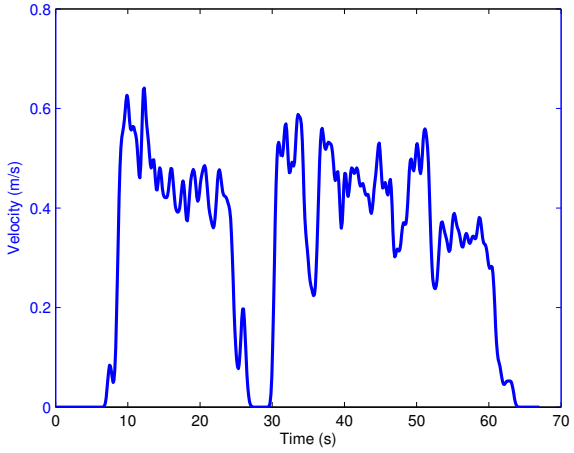

(a)

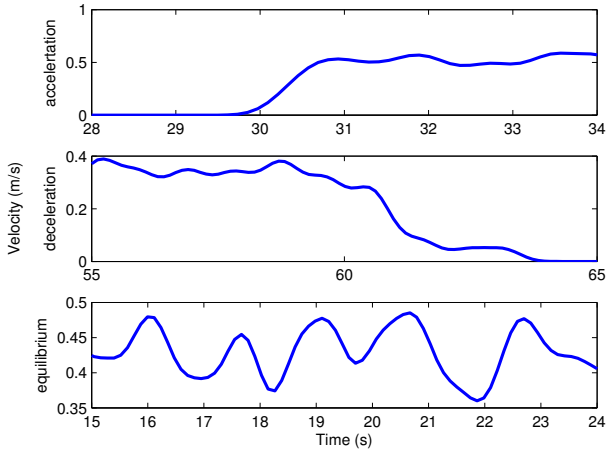

(b)

Fig.11 Experiment results. (a) The whole walking dynamic process (about one minute) with acceleration motion, deceleration motion and uniform motion. (b) Part views of the acceleration motion, deceleration motion and uniform motion are shown from top to bottom.

VI. Conclusion

In this paper, a 3D interactive virtual reality shopping market system was developed. The subject walks on the treadmill at will. The treadmill and 3D display adjust to the subject's intended walking speed, correspondingly. There are two main characters of the developed virtual market system. The first is treadmill velocity control which only uses force measurements. Compared with the previous treadmill-style locomotion methods, the proposed speed control in this paper shows great effectiveness and real-world applicability. The second is 3D display by which the subject gets a more immersive and realistic feeling. The future work is to connect the virtual shops with the real ones. In this way, the elderly person can healthily order goods in VR worlds at home.

Acknowledgment

This paper received constructive suggestions from Hisahito Noritake, Yusuke Taki and Shouichi Katou. The authors also would like to thank Haifeng Dong of the Arizona State University USA for proofreading.

References

[1] B. C. B. Yip and D. W. K. Man, "Virtual reality (VR) based community living skills training for people with acquired brain injury: a pilot study," *Brain Injury*, vol. 23, pp. 1017-1026, 2009.

[2] M. Farber, F. Hummel, C. Gerloff et al., "Virtual reality simulator for the training of lumbar punctures," *Methods of Information in Medicine*, vol. 48, pp. 493-501, 2009.

[3] D. Van, R. Hunneman and S. Wildlevuur, "Self city: training social skills in a game," in *2nd European Conf. Games-Bases Learning*, 2008, pp. 481-488.

[4] J. M. Hollerbach, "Locomotion interfaces and rendering," in *Haptic Rendering: Foundations, Algorithms, and Applications*, A. K. Peters, pp. 83-92, 2008.

[5] J. M. Hollerbach, "Locomotion interfaces," in *Handbook of virtual environments: design, implementation, and application*, Lawrence Erlbaum Associates, pp. 239-254, 2002.

[6] H. Noma and T. Miyasato, "Design for locomotion interface in a large scale virtual environment ATLAS: ATR locomotion interface for active self motion," in *7th Annual Symposium on Haptic Interface for Virtual Environments and Teleoperated Systems*, 1998, pp. 111-118.

[7] R. P. Darken and W. R. Cockayne, "The omni-directional treadmill: a locomotion device for virtual worlds," in *Proceedings of the 10th Annual ACM Symposium on User Interface Software and Technology*, 1997, pp. 213-221.

[8] H. Iwata and Y. Yoshida, "Path reproduction tests using a Torus treadmill," *Teleoperators and Virtual Environment*, vol 8, pp. 587-597, 1999.

[9] R. Christensen, J. M. Hollerbach, Y. Xu, et al., "Inertial force feedback for the Treadport locomotion interface," *Teleoperators and Virtual Environments*, vol. 9, pp. 1-14, 2000.

[10] J. M. Hollerbach, Y. Xu, R. Christensen, et al., "Design specifications for the second generation Sarcos Treadport locomotion interface," in *Proceedings of ASME Dynamic Systems and Control Division*, DSC-vol. 69-2, 2000, pp. 1293-1298.

[11] Instrumented Treadmill User Manual (Version 3.3), Bertec Corporation, 2008.